Breaking MAD

joint constraints on the anisotropy and mass profiles of massive elliptical galaxies

Shawn Knabel, Tommaso Treu, Chih-Fan Chen
University of California, Los Angeles

Sections of the Presentation

Section 1: Background and Motivation

Section 2: Observations and Kinematics

Breaking MAD

Section 3: Dynamical Modeling

Tension in H_0 needs to be resolved

Early- and Late-Universe probes disagree

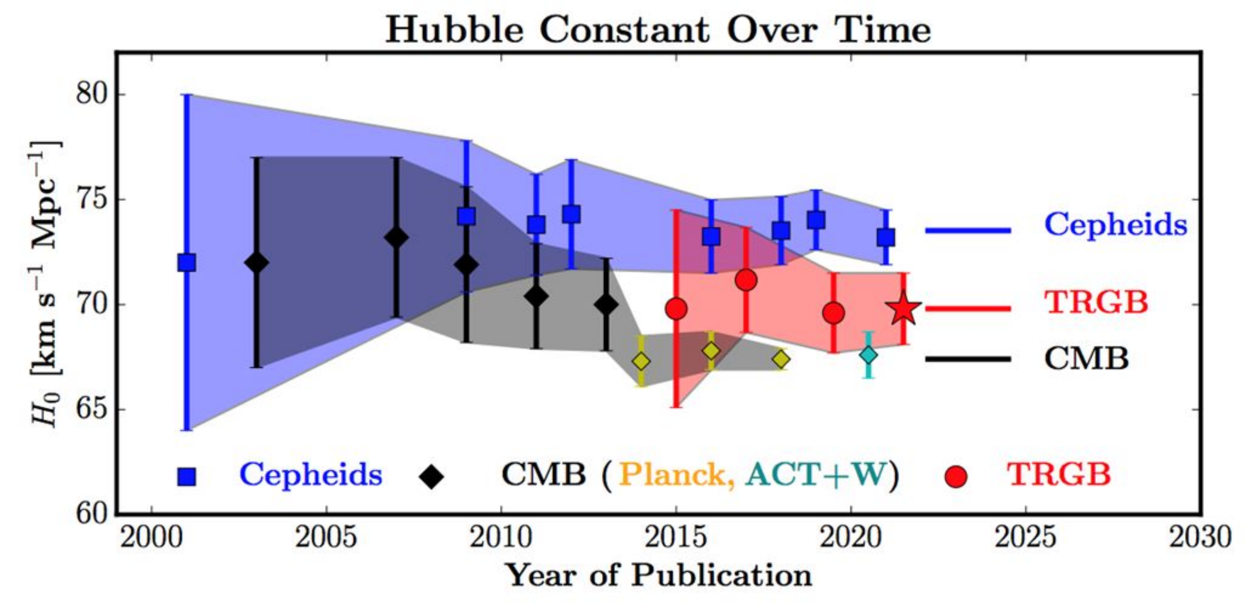

Freedman et al. 2021

Tension in H_0 can be resolved with time-delay cosmography

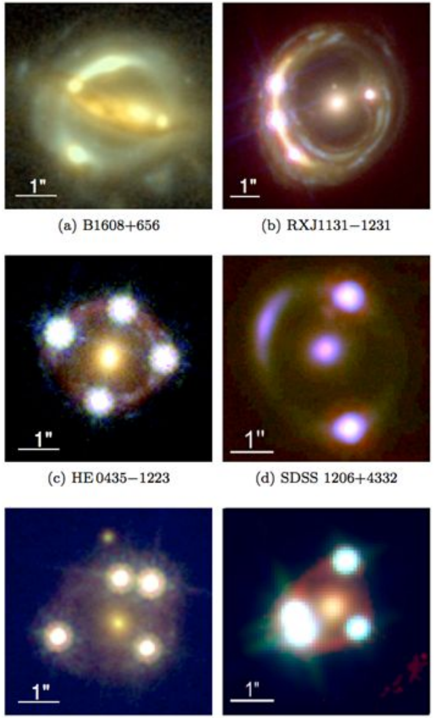

(a) B1608+656 (b) RXJ1131−1231
(c) HE 0435−1223 (d) SDSS 1206+4332
(e) WFI2033−4723 (f) PG 1115+080

Wong et al. 2019

Independent measurement with simple physics

Time-delay distance is an absolute cosmological distance… inversely proportional to H_0

Tension in H_0 can be resolved with time-delay cosmography

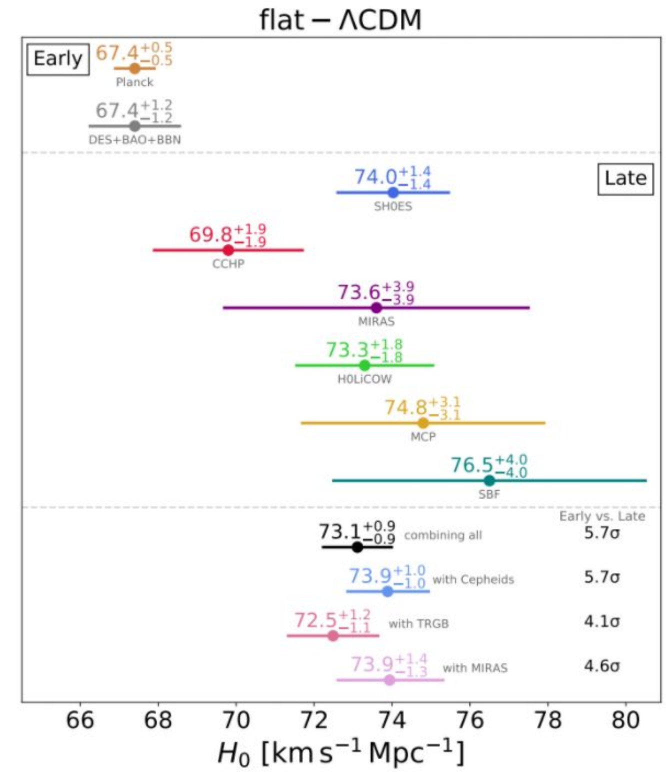

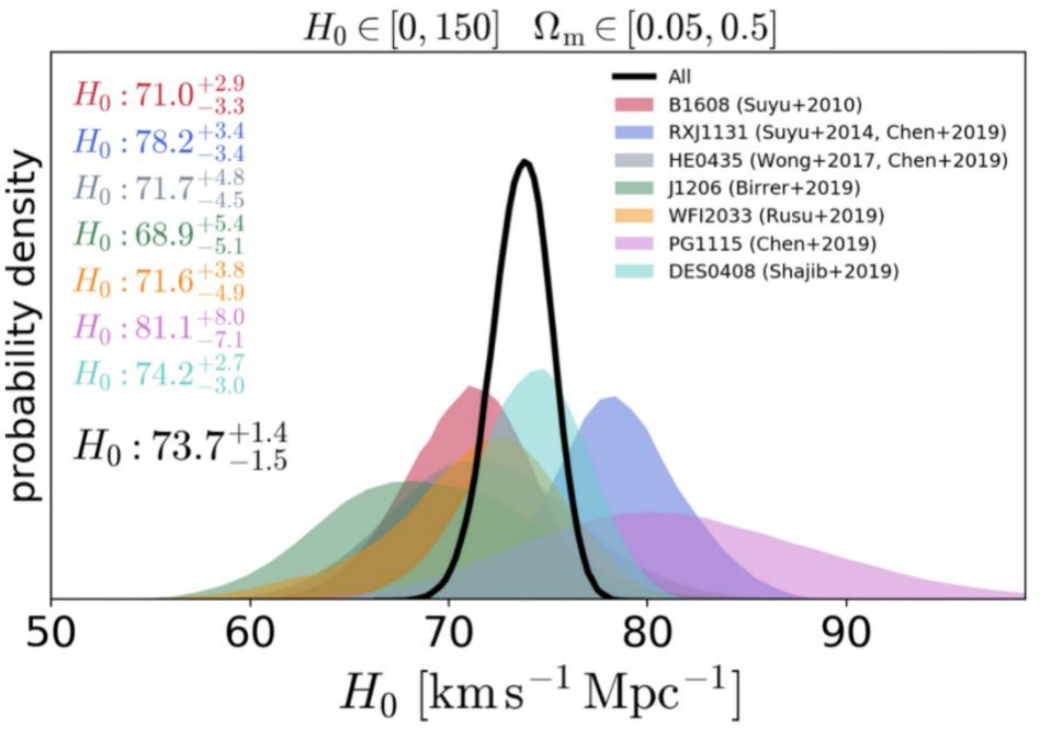

Verde, Treu and Riess 2019

Wong et al. 2019

Ingredients for H_0 are few

1. Time delay between arrival of quasar images
2. Lensing potential between quasar images in lens plane

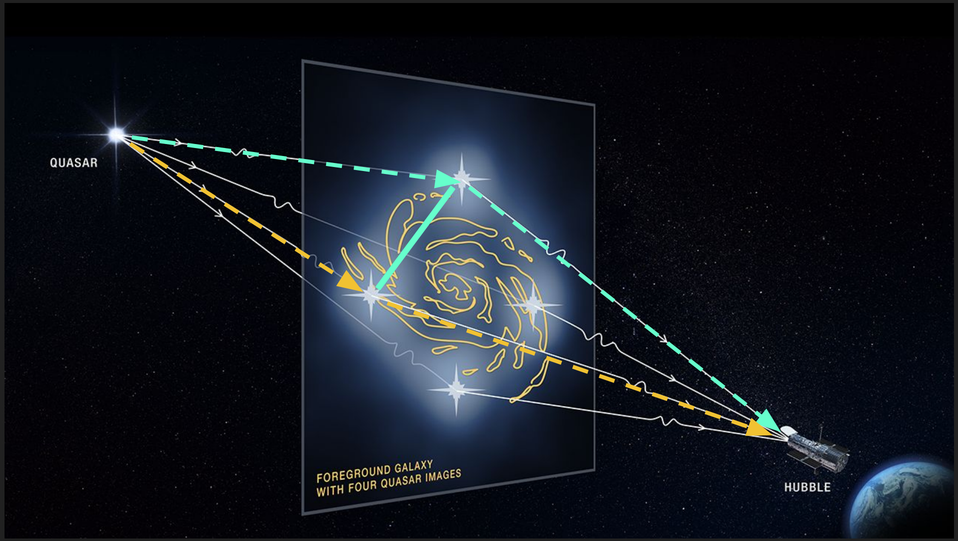

NASA, ESA, and D. Player (STScI)

A Tale of Two Degeneraci(ti)es

1. MSD Mass-Sheet Degeneracy (or Transform - “MST”)
2. MAD Mass-Anisotropy Degeneracy

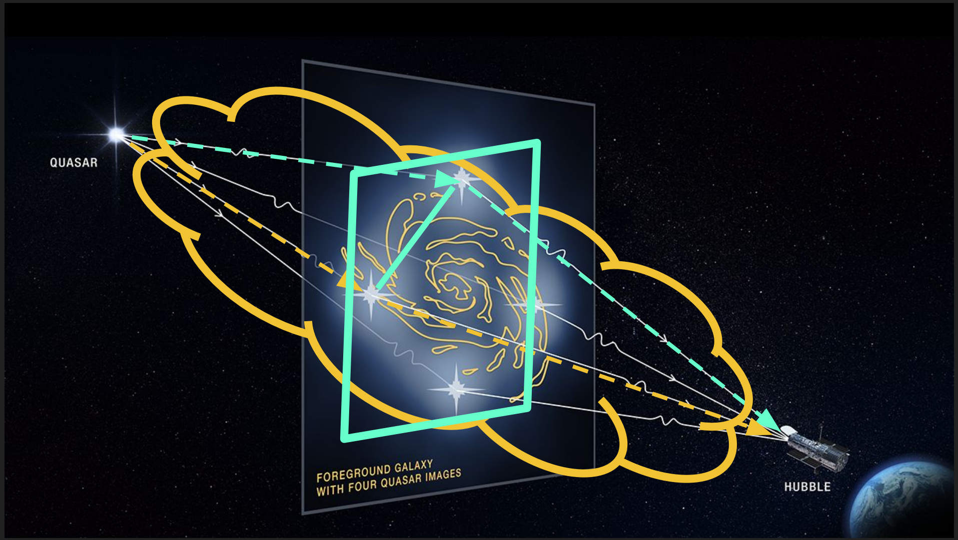

NASA, ESA, and D. Player (STScI)

The infamous Mass-Sheet Transform (Degeneracy)

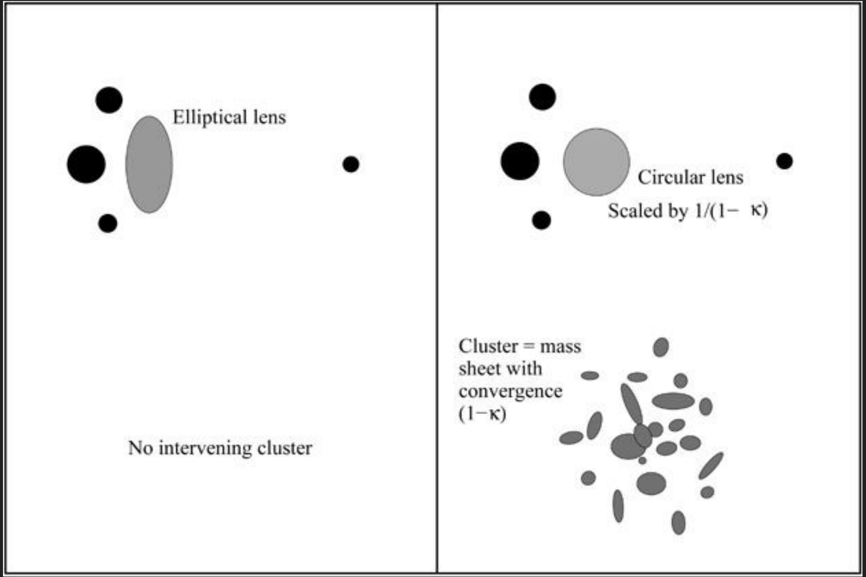

F. Corbin 2003

$$\kappa_\lambda(\theta) = \lambda \times \kappa(\theta) + (1 - \lambda)$$

Two contributors to MST:

1. External l.o.s. structure
2. Internal mass profile

Ingredients for H_0 are still few

We need:

1. Time delay
2. Lensing potential
3. External MST
4. Internal MST

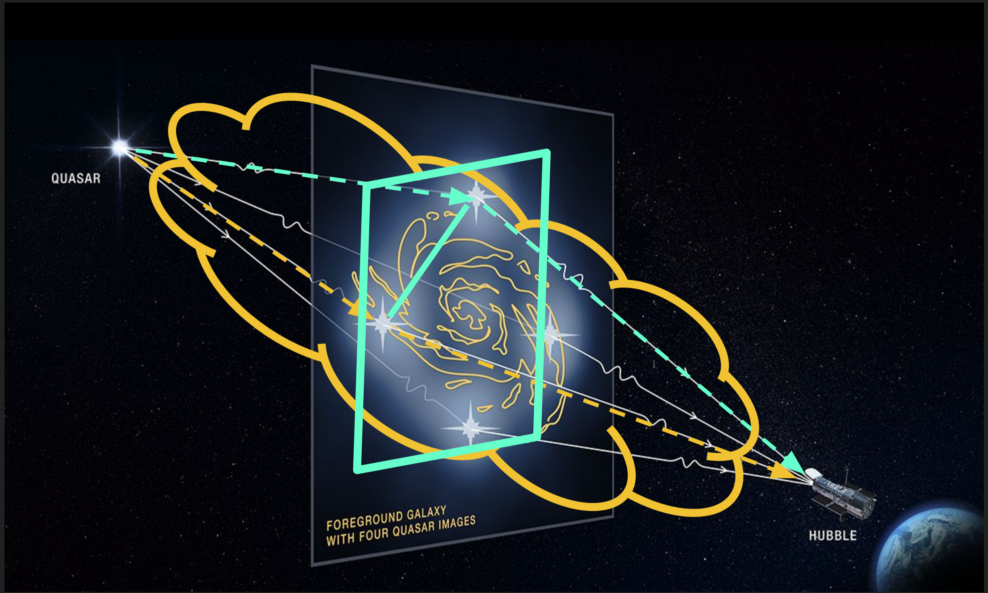

NASA, ESA, and D. Player (STScI)

Ingredients for H_0 are observable

1. Time delay - photometry
2. Lensing potential - lens modeling
3. External MST - weak lensing/simulations
4. Internal MST - …

Mass density profile assumptions

or

Lensing-independent tracers of gravitational potential

We want to account for maximal possible effects of MST

We want empirical constraints over theoretical assumptions

A dynamical mass from stellar kinematics allows us constrain the mass profile and the effects of the internal MST on the uncertainties of inferred quantities (H_0)

Stellar anisotropy can be constrained with spatially resolved kinematics

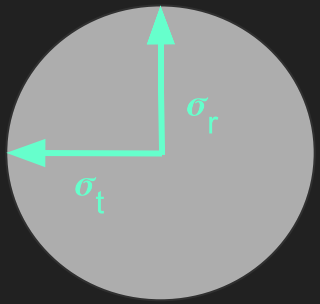

Isotropic

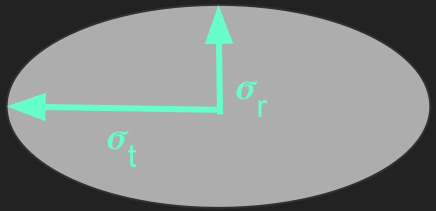

Anisotropic

How *not isotropic* the stellar velocity ellipsoid is

$$\beta_{\rm ani}(r) \equiv 1 - \frac{\sigma_{\rm t}^2(r)}{\sigma_{\rm r}^2(r)}$$

For isotropic (spherical ellipsoid) case, $\boldsymbol{\beta}_{\rm ani} = 0$

Kinematics of distant time-delay lenses are difficult to get

NASA, ESA, A. Nierenberg (JPL) and T. Treu

Limited by the S/N possible for the individual lenses

Kinematics of other *closer* lenses are *less* difficult to get

Constraints on mass profiles of the larger population of lensing elliptical galaxies

Bayesian hierarchical modeling connects the individuals and population

Constrain MAD

Constrain MSD

Constrain H_0

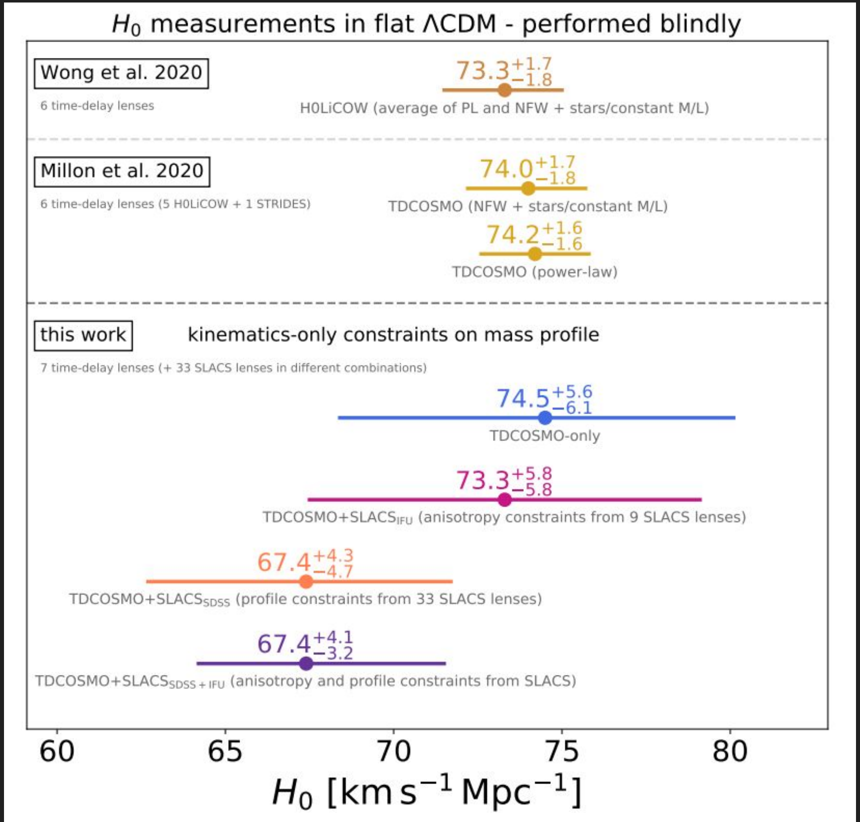

S Birrer et al. 2020

Keck KCWI IFU spectroscopy measures spatially-resolved kinematics

Integral-Field Units (IFU) measure a spectrum at each pixel

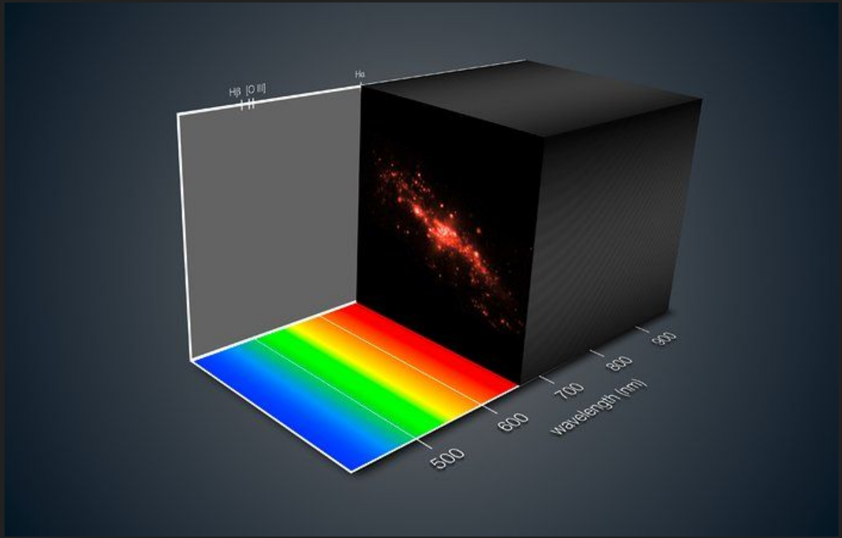

ESO/MUSE consortium/R. Bacon/L. Calçada

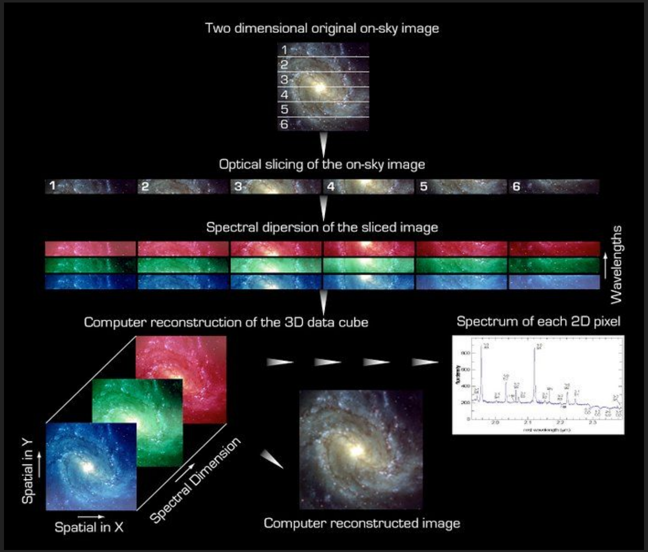

ESO

Keck is also good for writing music.

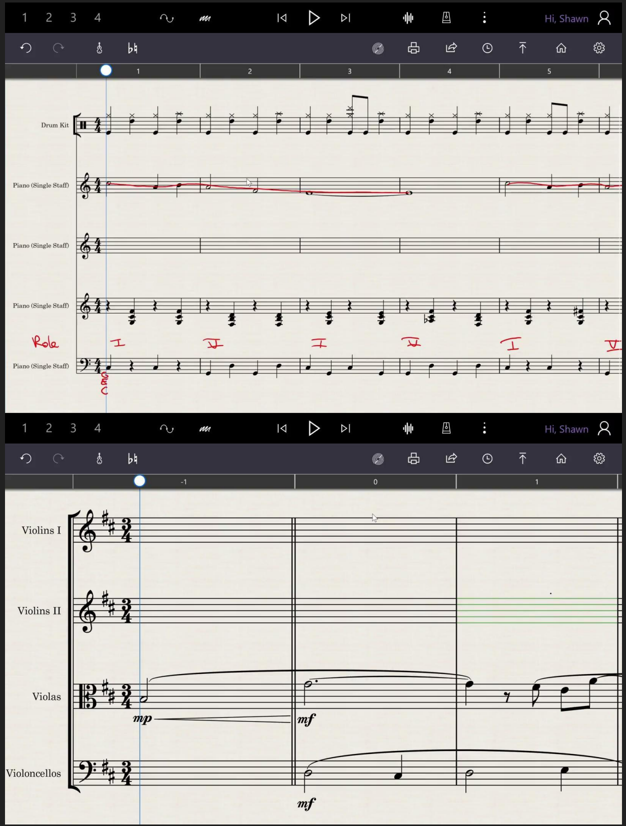

Knabel et al. in prep

In spite of myself… all 14 SLACS lenses were observed

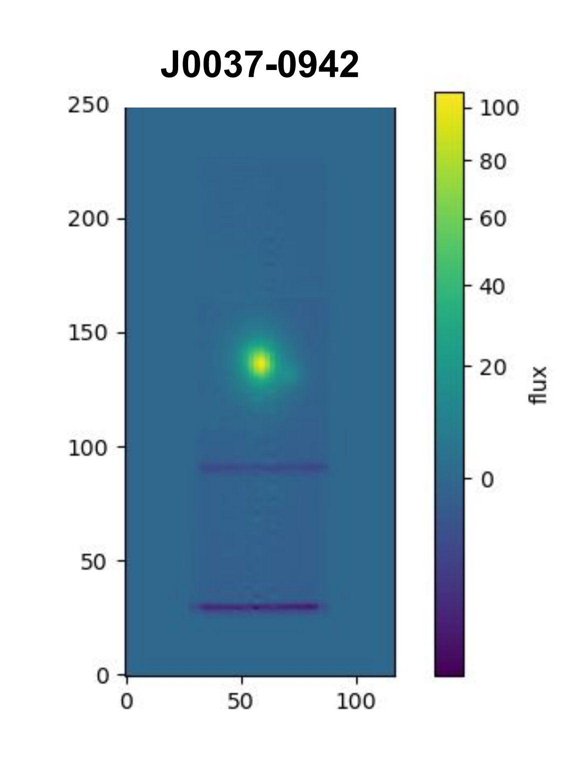

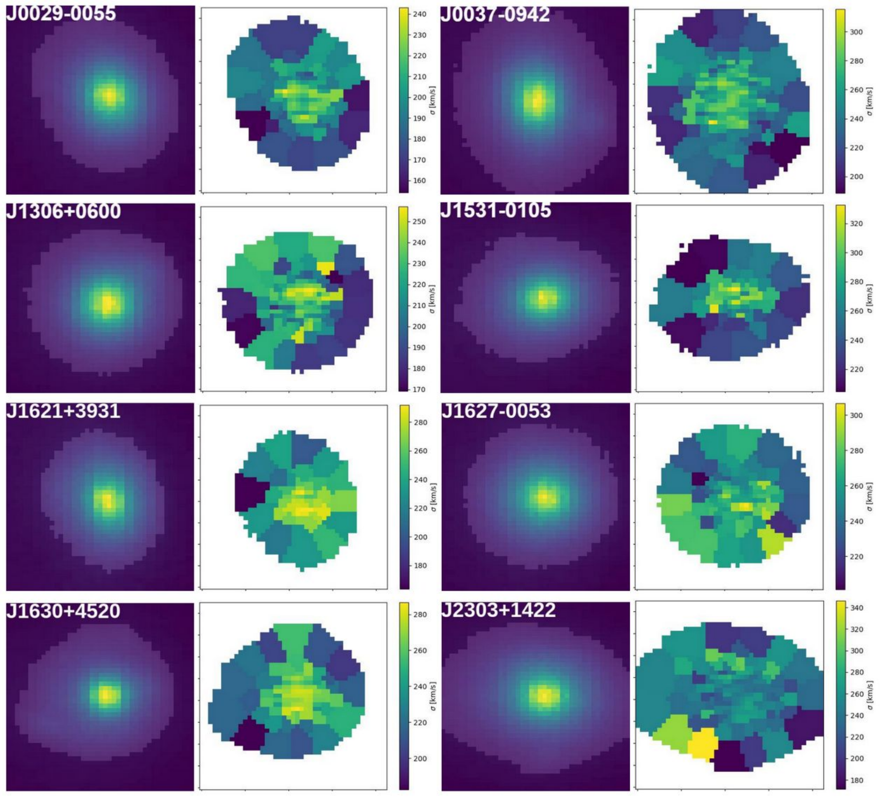

Knabel et al. in prep

Pixels are binned to regions of similar S/N for comparison

Voronoi binning bins to designated target S/N (e.g. 10-20)

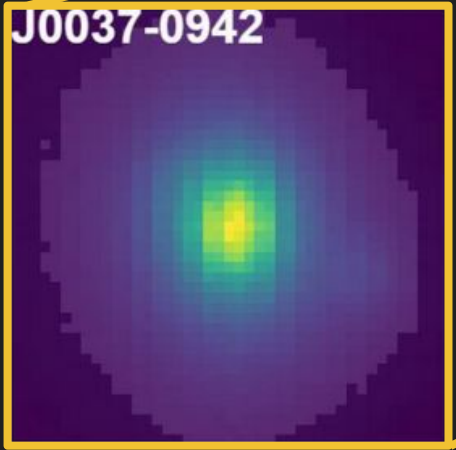

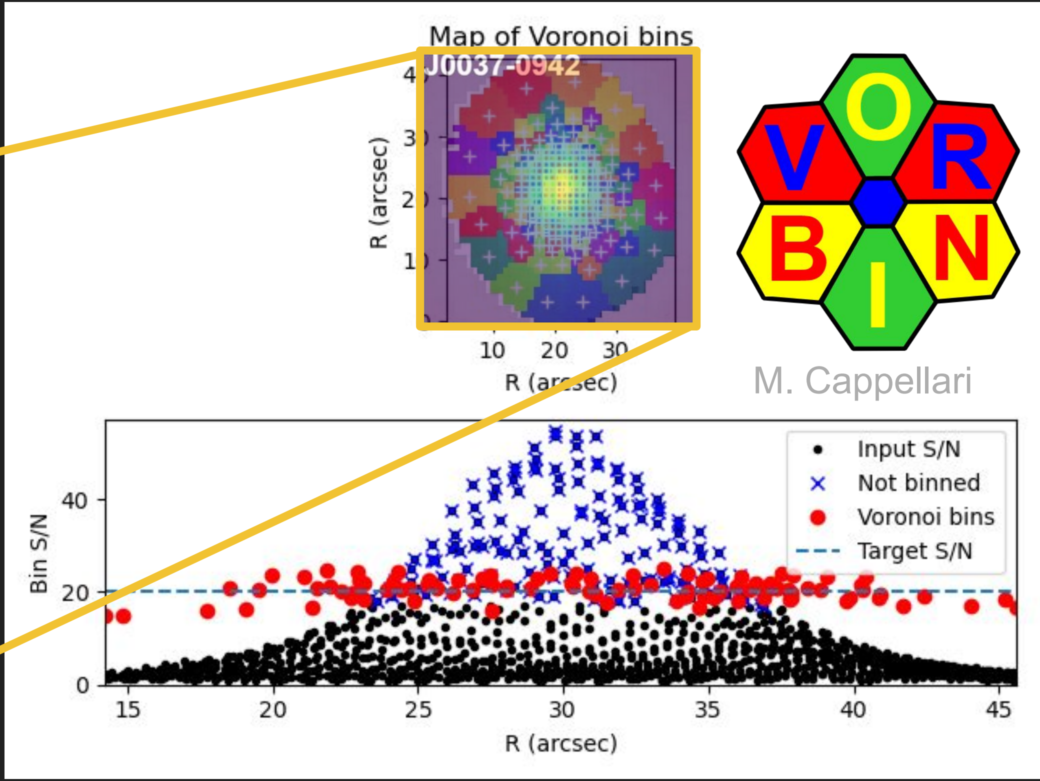

Knabel et al. in prep

Penalized Pixel Fitting (pPXF)

Generate kinematic maps by fitting with stellar spectrum templates and adjusting linewidths

XSL team

M. Cappellari

Ca II H&K absorption lines are fit to measure kinematics

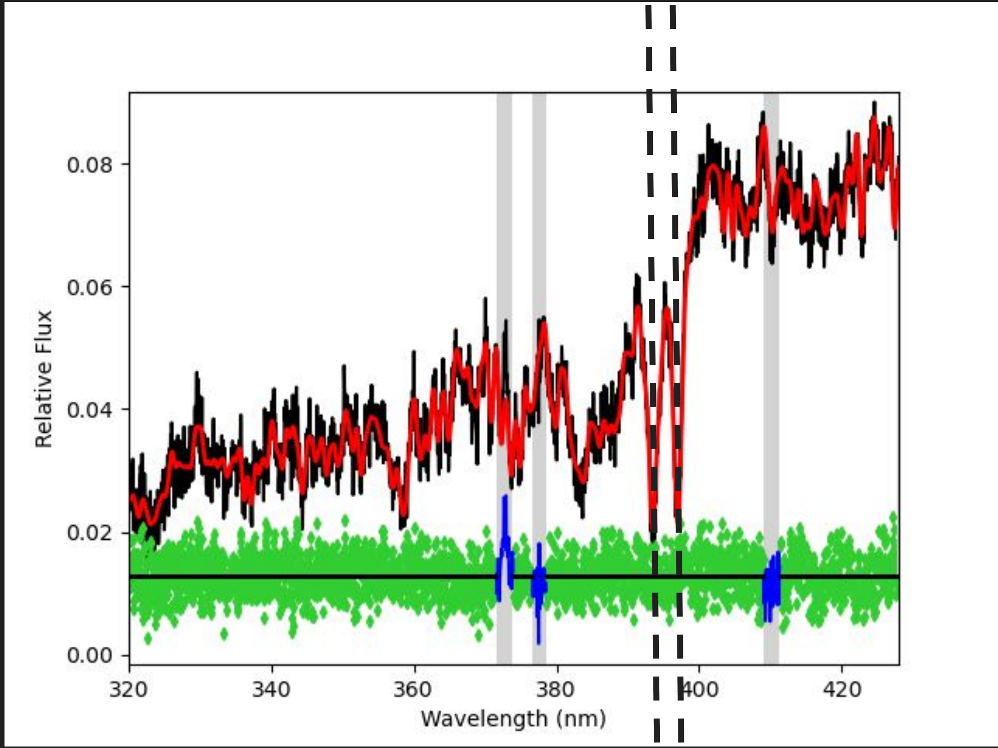

Line centers, widths, and amplitudes are scaled to fit the composite spectra in each bin

Knabel et al. in prep

2-D kinematic maps describe projection of stellar motion

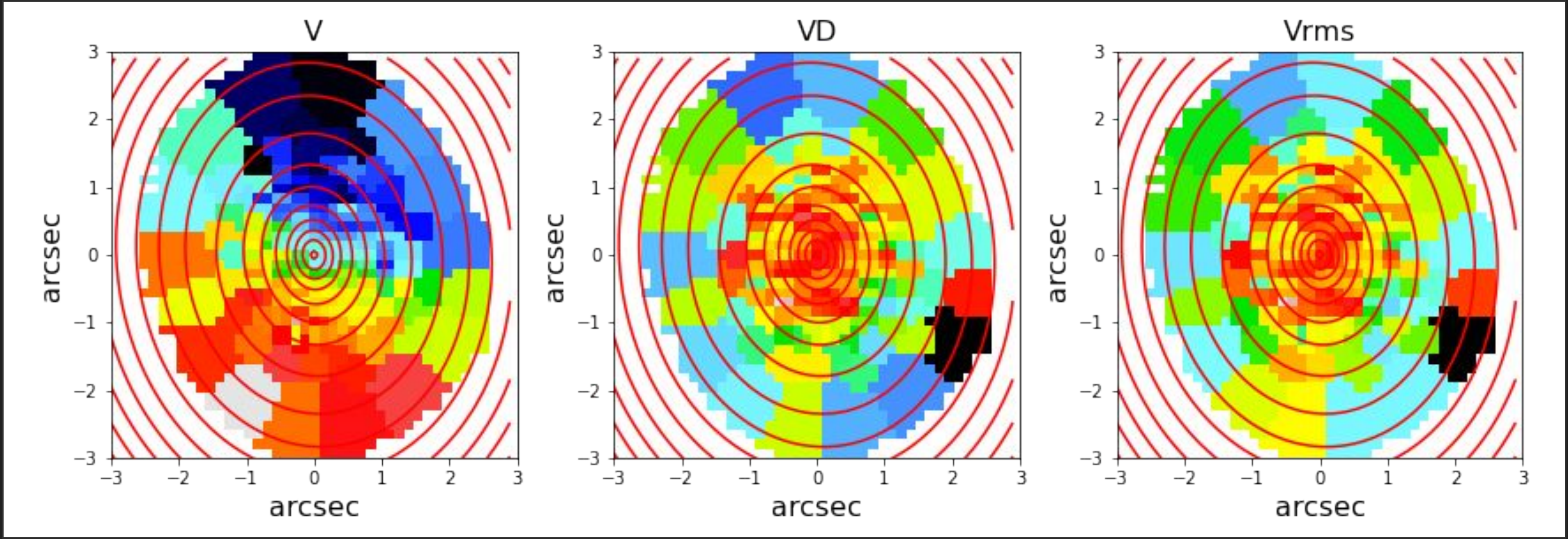

Knabel et al. in prep

The Jeans equation connects kinematics and dynamics

Jeans Anisotropic Modeling (JAM) solves the Jeans equation allowing for orbital anisotropy in axisymmetric or spherical alignment to dynamically describe the radial mass profiles of elliptical galaxies

M. Cappellari

Surface brightness profile is tracer of stellar mass

Multi-Gaussian Expansion (MGE) approximates the surface brightness with Gaussian components

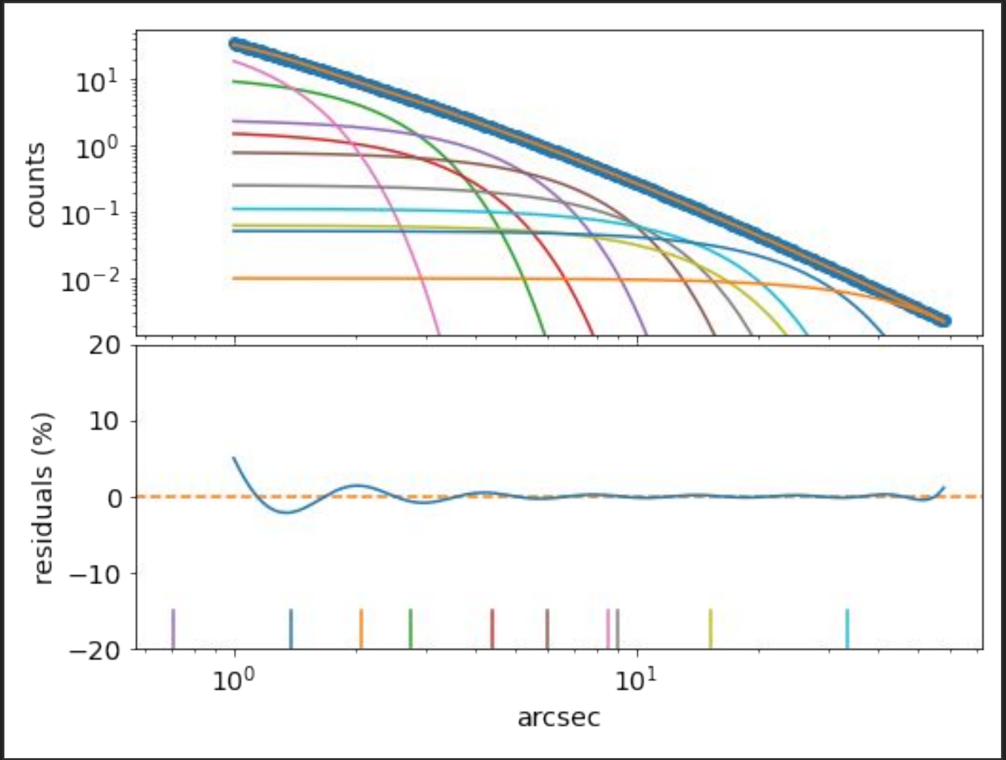

Knabel et al. in prep

Fitting photometry of the datacube is inadvisable…

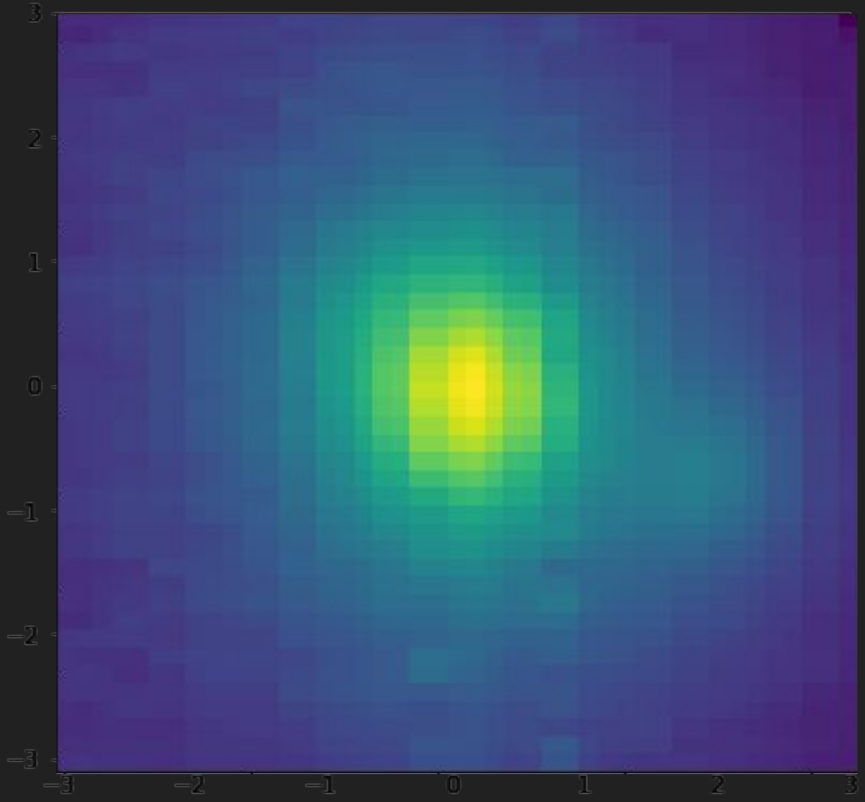

Knabel et al. in prep

Initial fit to central ellipse for ellipticity and position angle

Informs the construction of the Gaussian components

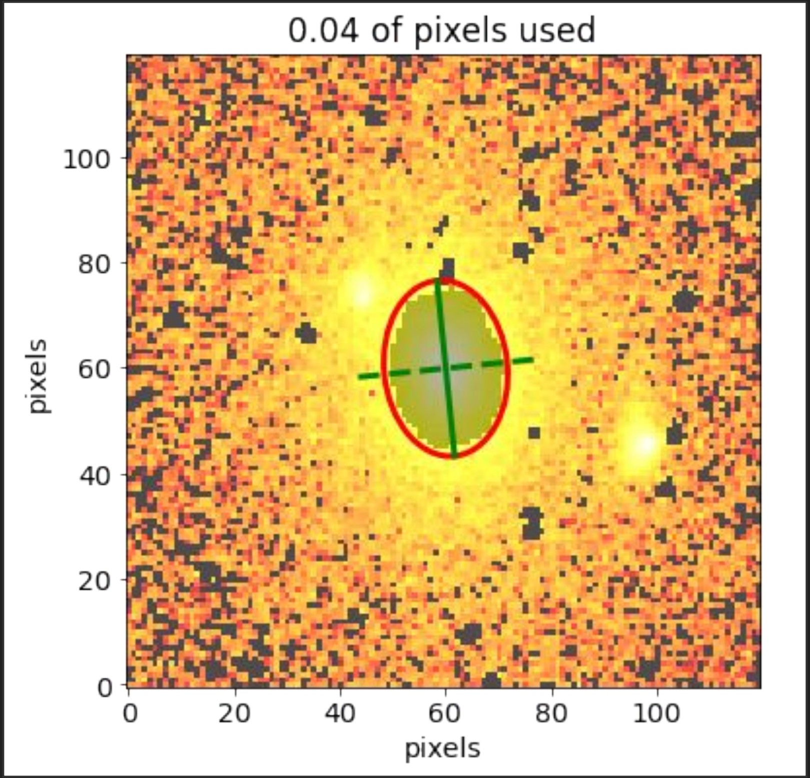

Knabel et al. in prep

Photometry is binned to evenly space sectors about center

Guides the construction of the Gaussian components

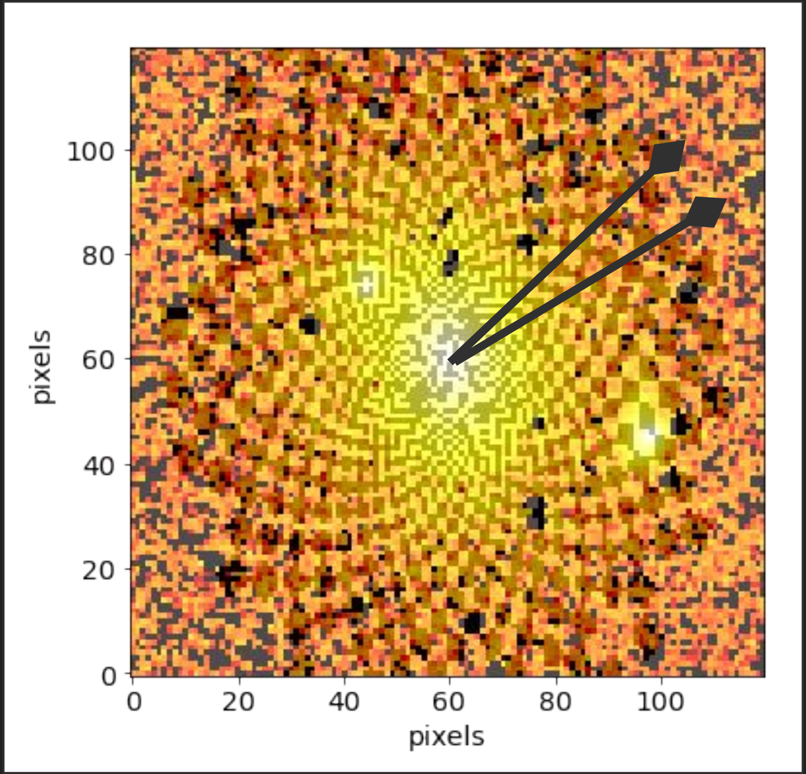

Knabel et al. in prep

Multi-Gaussian Expansion fits sector-binned photometry

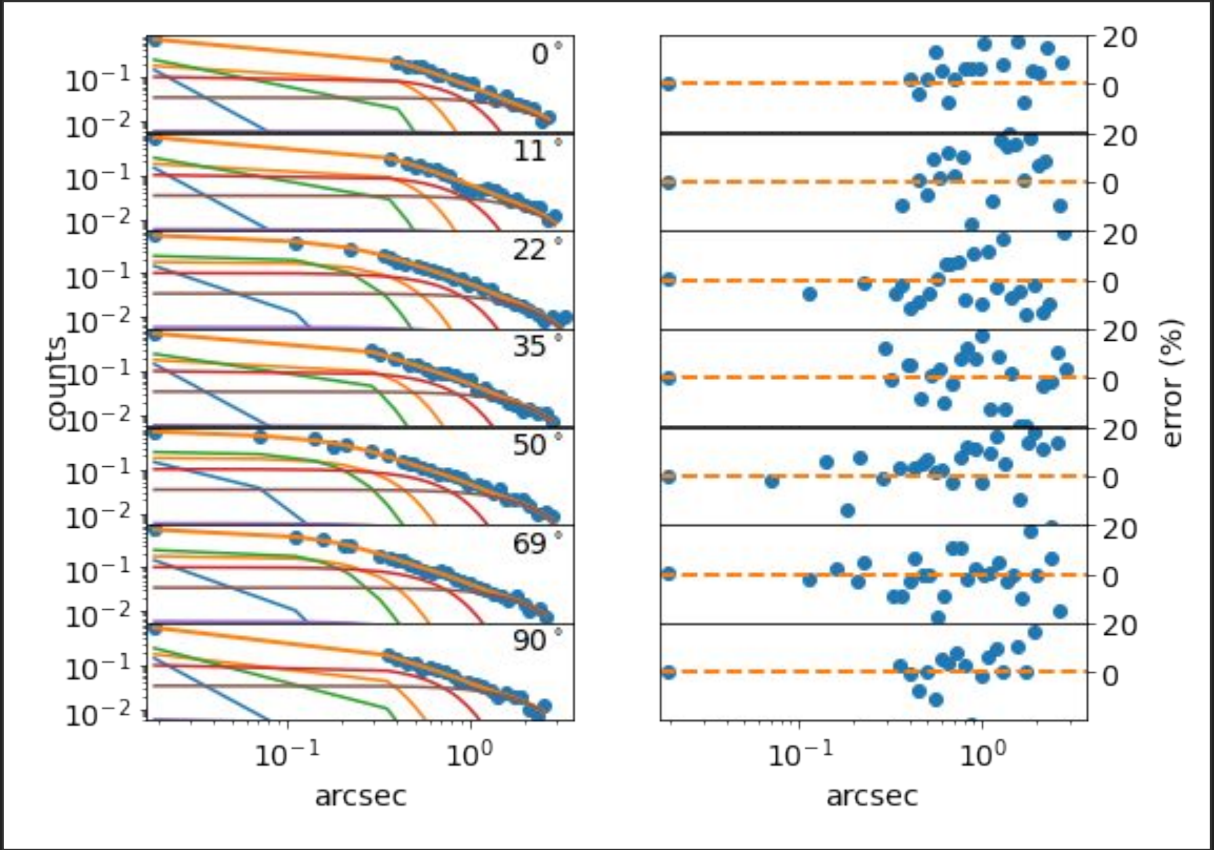

Knabel et al. in prep

Multi-Gaussian Expansion fits sector-binned photometry

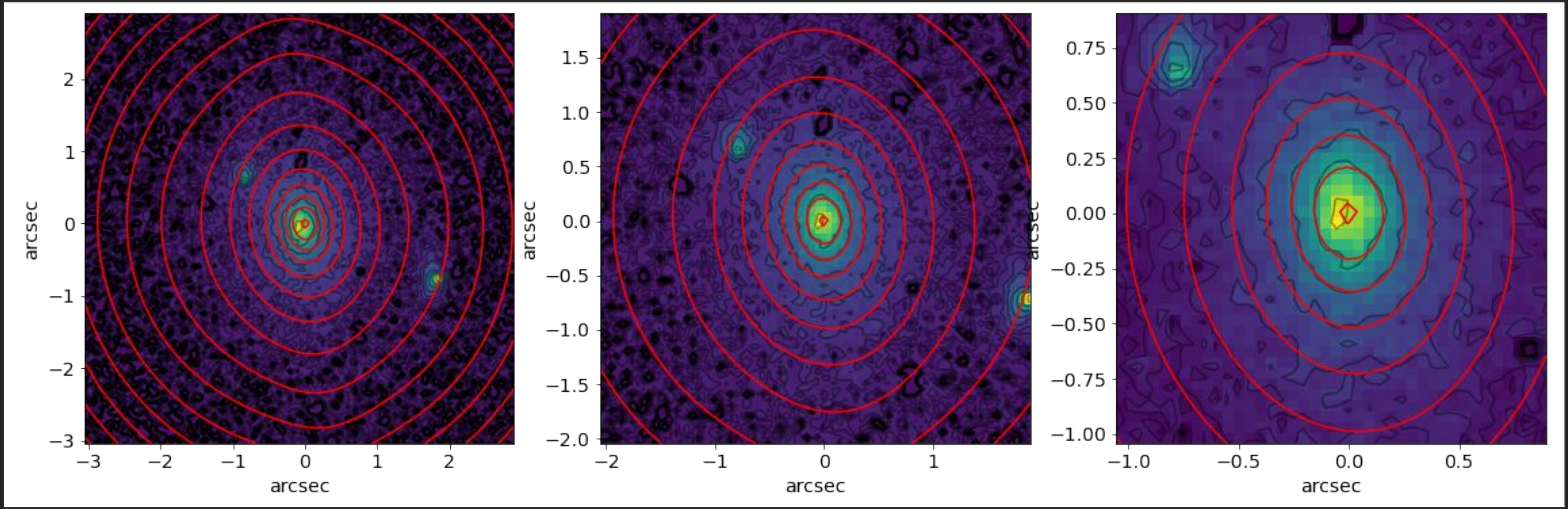

Knabel et al. in prep

We fit for the best *roundest* isophotes and simplest model

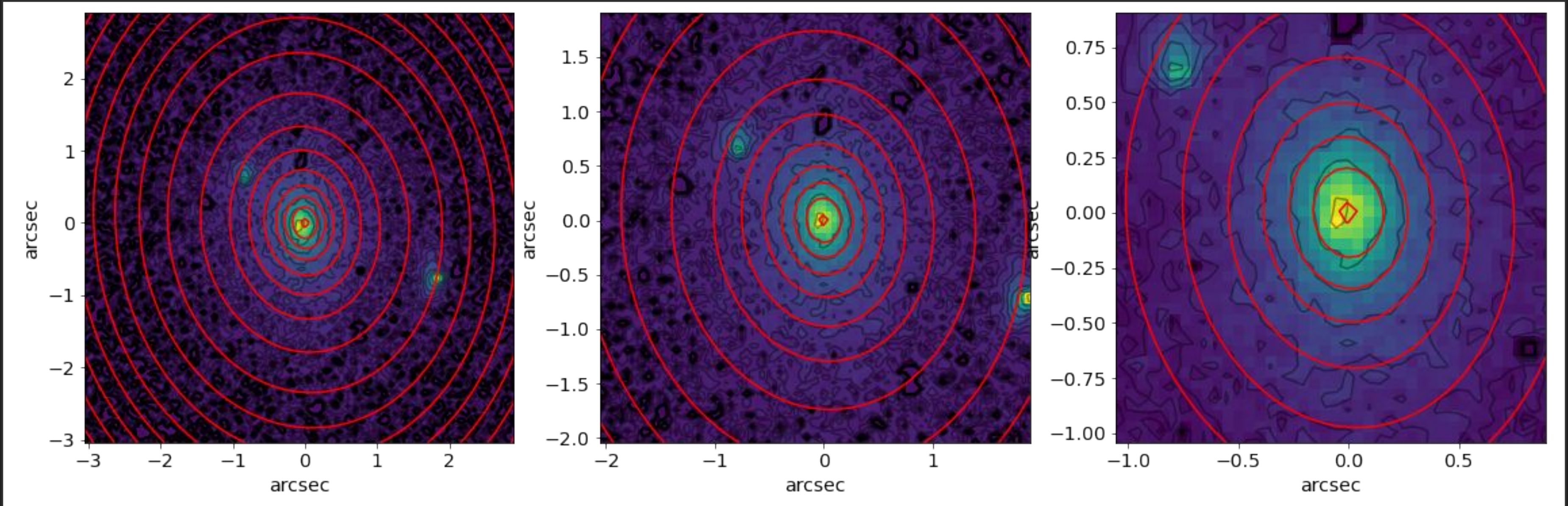

Knabel et al. in prep

We check alignment of kinematic and photometric axis

Aligned with kinematics

Aligned with photometry

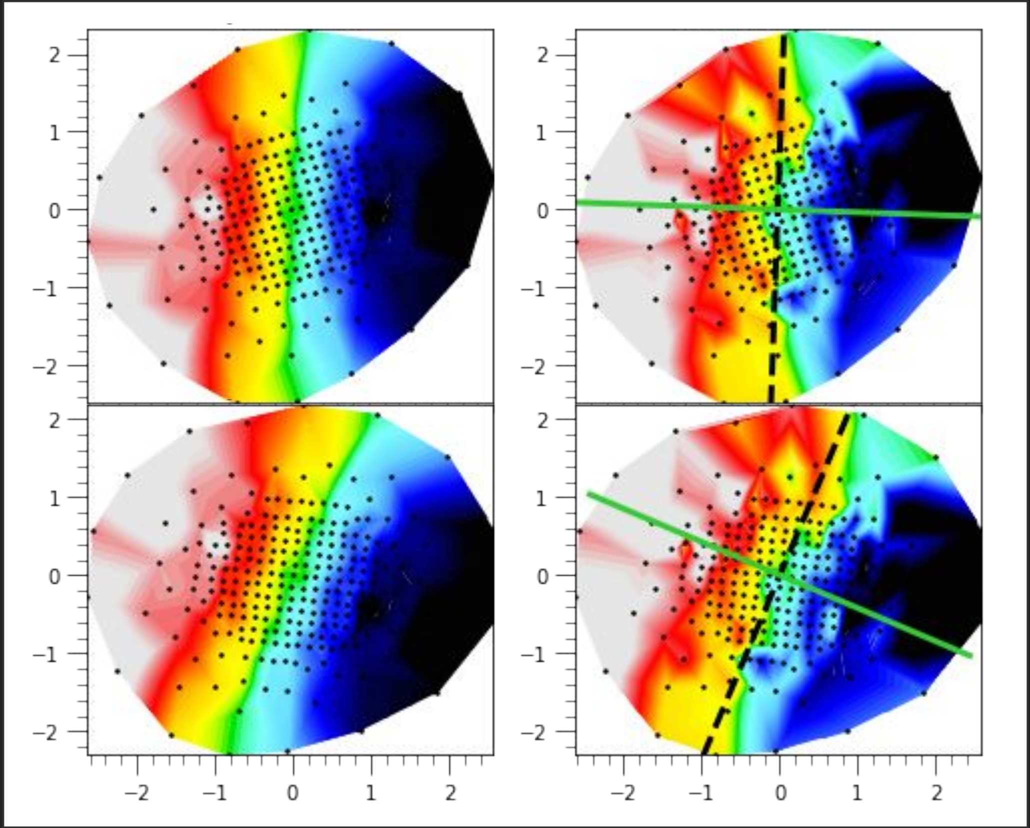

Knabel et al. in prep

Each Gaussian component is assigned an anisotropy β_k

Each Gaussian k contributes most strongly at r = σ_k , so each β_k can be assigned according to any profile of anisotropy $\beta(r)$

$$\beta_{\rm ani}(r) \equiv 1 - \frac{\sigma_{\rm t}^2(r)}{\sigma_{\rm r}^2(r)}$$

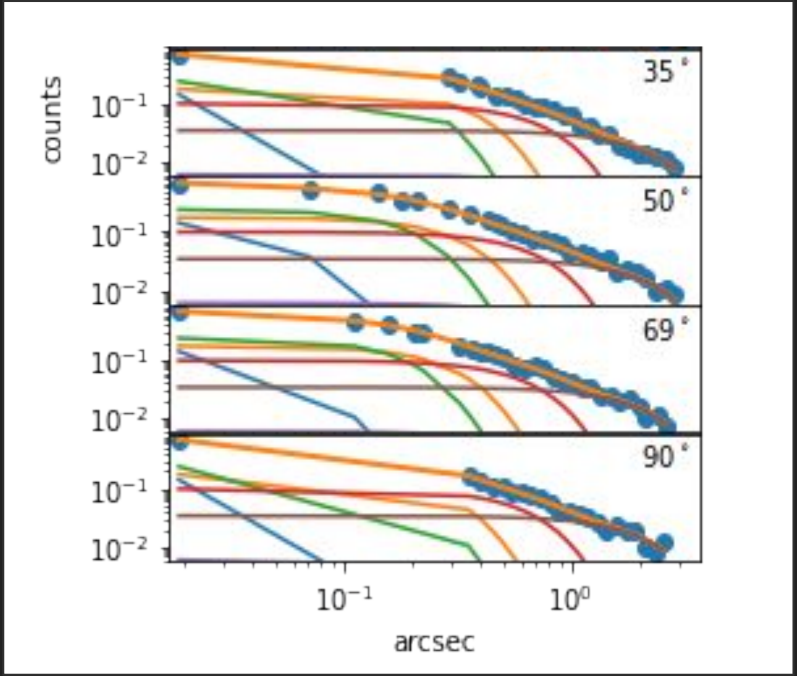

Knabel et al. in prep

We consider four different possible radial profiles $\beta(r)$

1. Constant
2. Osipkov-Merritt (OM)
3. Modified OM
4. Inner/Outer

$$\beta_{\rm ani}(r) \equiv 1 - \frac{\sigma_{\rm t}^2(r)}{\sigma_{\rm r}^2(r)}$$

$$Beta(r) = \frac{r^2}{r_{ani}^2 + r^2} = \frac{1}{a_{ani}^2(r_{eff}/r)^2 + 1}$$

$$a_{ani} = r_{ani}/r_{eff}$$

Osipkov-Merritt Model has been historically used $\beta(r)$

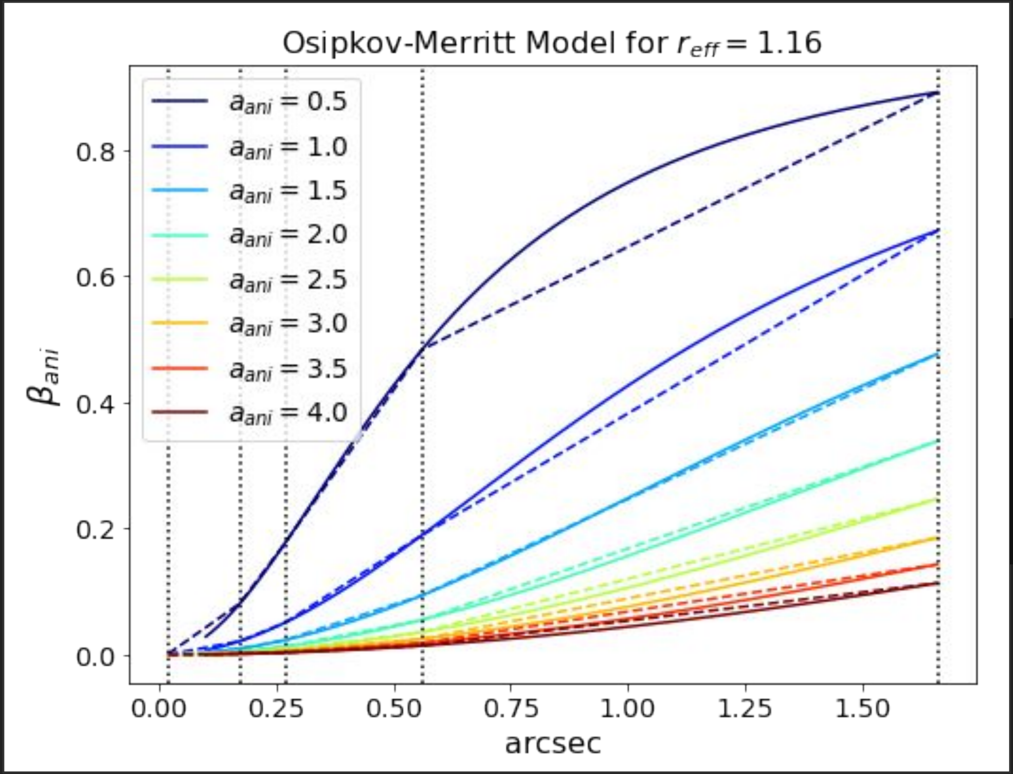

$$\beta_{\mathrm{ani}}(r) \equiv 1 - \frac{\sigma_{\mathrm{t}}^2(r)}{\sigma_{\mathrm{r}}^2(r)}$$

$$Beta(r) = \frac{r^2}{r_{ani}^2 + r^2} = \frac{1}{a_{ani}^2 (r_{eff}/r)^2 + 1}$$

$$a_{ani} = r_{ani}/r_{eff}$$

Knabel et al. in prep

Light-follows-mass gives first dynamical mass estimate

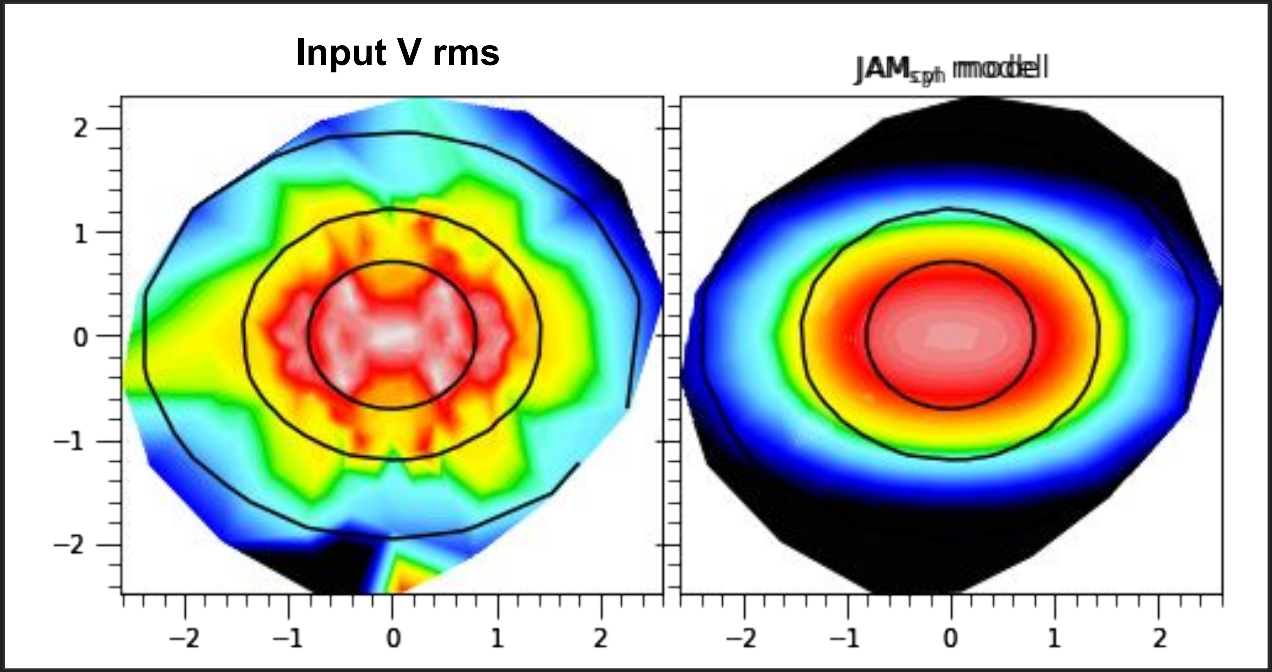

Knabel et al. in prep

Total mass 4.786e+11 $M_\odot$

The first velocity moment helps validate but isn't necessary

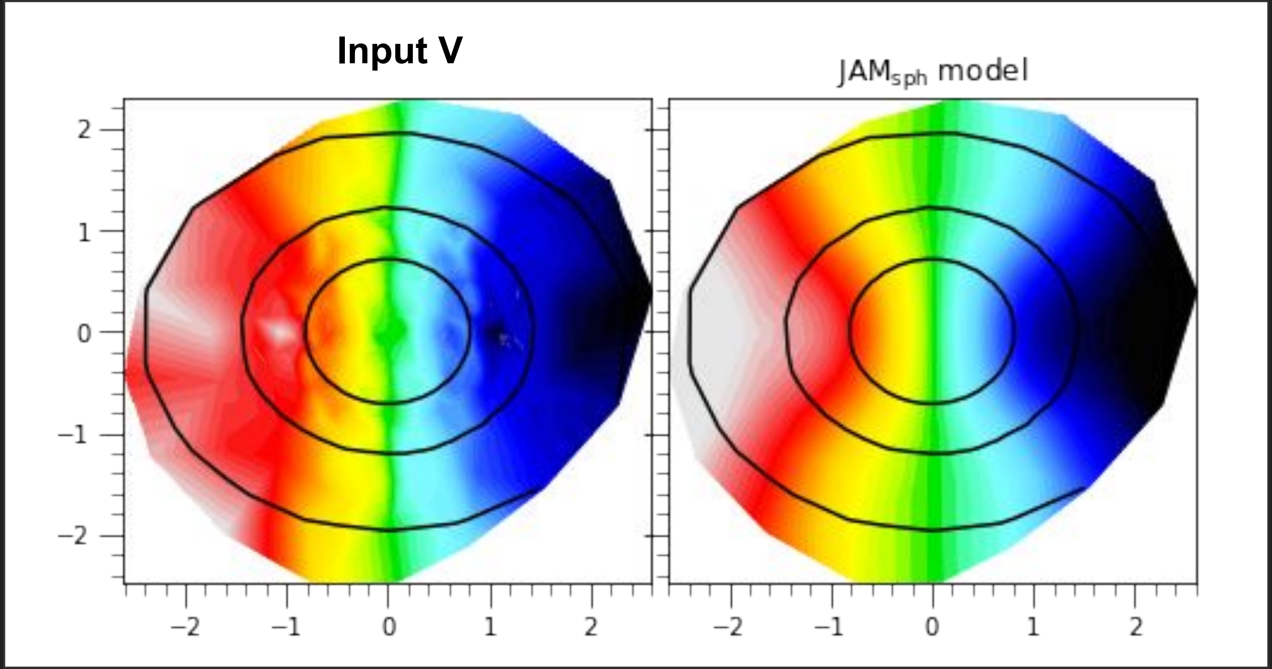

Knabel et al. in prep

We consider three different mass models $\rho(r)$

1. Power law total mass
2. Stellar + NFW halo
3. Stellar + generalized NFW halo

$$\rho(r) \propto \left(\frac{r}{r_{break}}\right)^{\gamma}\left(1+\frac{r}{r_{break}}\right)^{-\gamma-3}$$

γ inner profile slope

r_{break} radius at which slope changes

Simplest fit – spherical alignment and constant anisotropy

AdaMet - Adaptive Metropolis Bayesian analysis package

Utilizing broad priors from fiducial values and previous light-follows-mass model

Simplest fit – 4 parameters for anisotropy and mass

1. q_{min}
2. σ_t/σ_r
3. f_{dm}
4. $\log(M/L)$

$\beta_{ani} \sim 0.256$

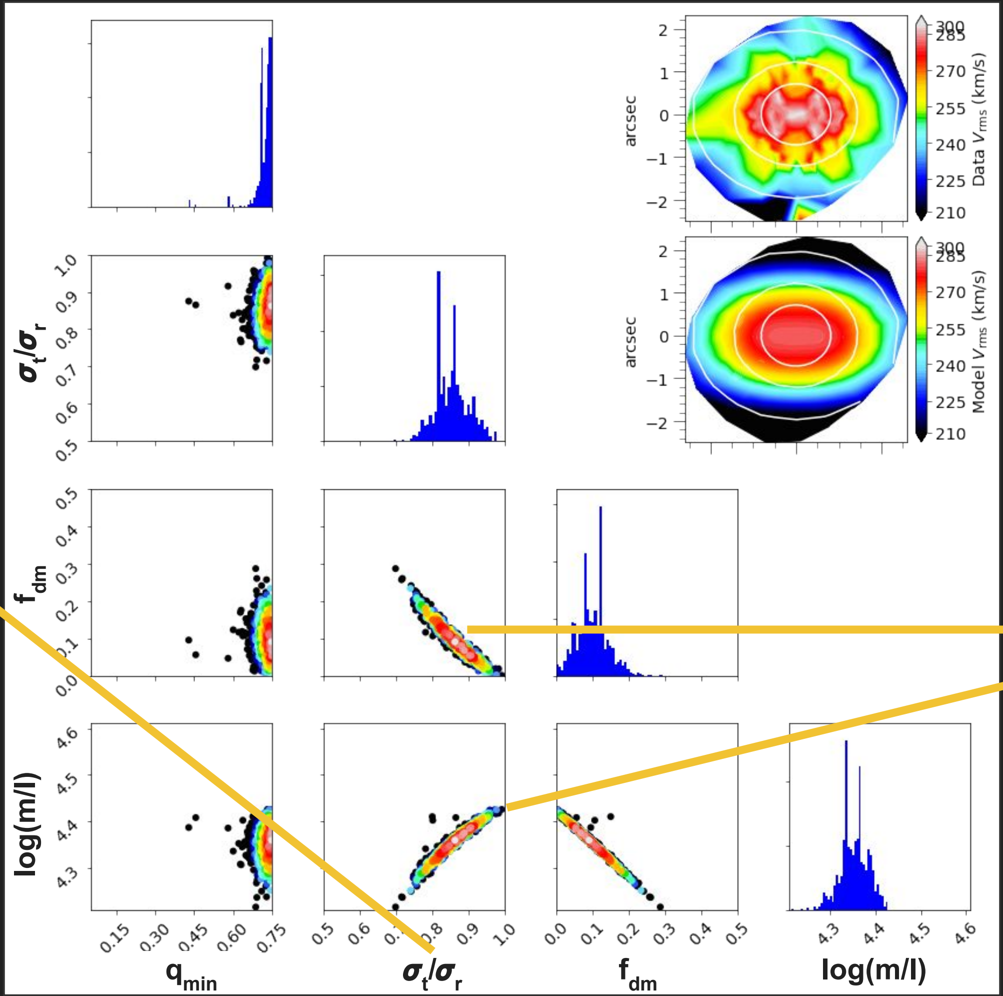

~~Breaking~~
MAD

Knabel et al. in prep

The total mass profile can be easily obtained

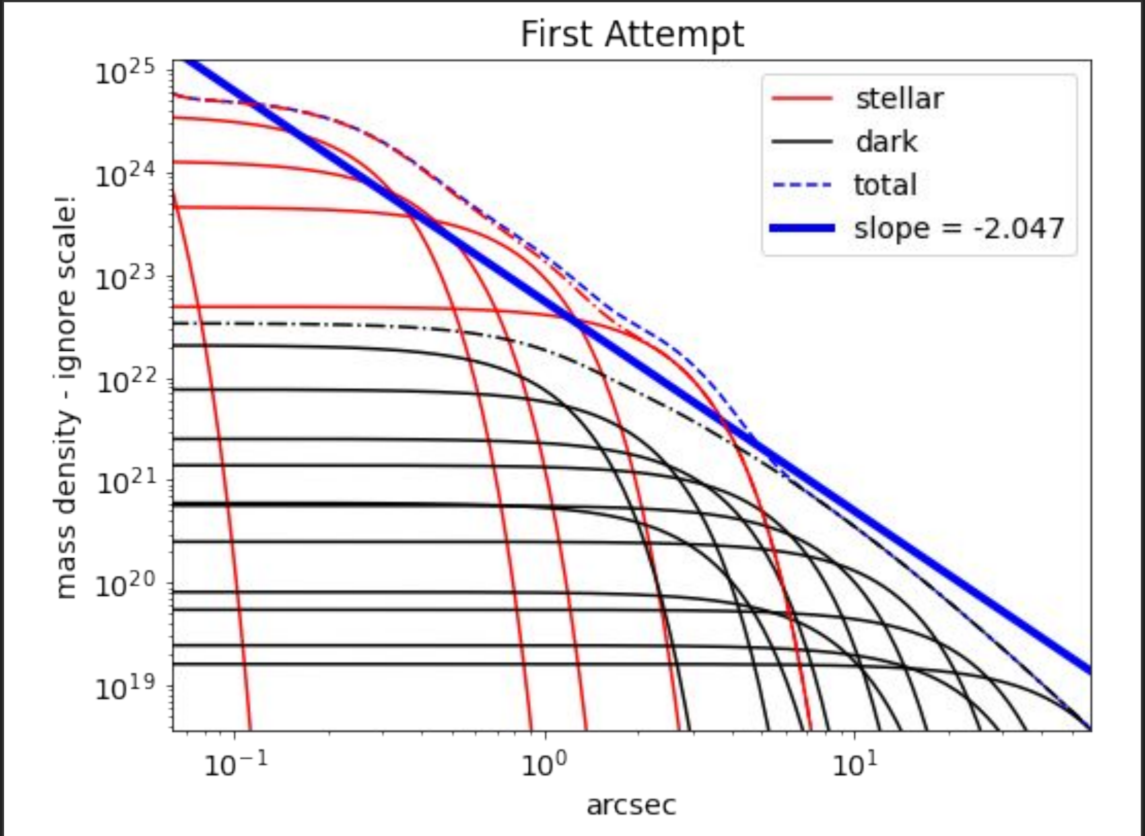

Knabel et al. in prep

But we get posteriors for $\boldsymbol{\beta}_{ani}$ and mass... best estimates:

Constant $\boldsymbol{\beta}_{ani}$ ~ 0.256

Breaking MAD

Power law slope $\boldsymbol{\gamma}$ ~ -2.047

In summary

Though currently in the beginning stages, our observations and analytical framework appear to be capable of addressing the MAD problem of the mass-anisotropy degeneracy.

This will help us get to 1% precision on H_0.

The relative arrival time between two images $\boldsymbol{\theta}_{\mathrm{A}}$ and $\boldsymbol{\theta}_{\mathrm{B}}$, Δt_{AB}, originated from the same source is

$$\Delta t_{\mathrm{AB}} = \frac{D_{\Delta t}}{c} \left(\phi(\boldsymbol{\theta}_{\mathrm{A}}, \boldsymbol{\beta}) - \phi(\boldsymbol{\theta}_{\mathrm{B}}, \boldsymbol{\beta}) \right), \tag{5}$$

where c is the speed of light,

$$\phi(\boldsymbol{\theta}, \boldsymbol{\beta}) = \left[\frac{(\boldsymbol{\theta} - \boldsymbol{\beta})^2}{2} - \psi(\boldsymbol{\theta}) \right] \tag{6}$$

is the Fermat potential (Schneider 1985; Blandford & Narayan 1986), and

$$D_{\Delta t} \equiv (1 + z_{\mathrm{d}}) \frac{D_{\mathrm{d}} D_{\mathrm{s}}}{D_{\mathrm{ds}}}, \tag{7}$$

The dynamics of stars with the density distribution $\rho_*(r)$ in a gravitational potential $\Phi(r)$ follows the Jeans equation. In this work, we assume spherical symmetry and no rotation in the Jeans modeling. In the limit of a relaxed (vanishing time derivatives) and spherically symmetric system, with the only distinction between radial, σ_{r}^2, and tangential, σ_{t}^2, dispersions, the Jeans equation results in (e.g., Binney & Tremaine 2008)

$$\frac{\partial(\rho_* \sigma_{\mathrm{r}}^2(r))}{\partial r} + \frac{2\beta_{\mathrm{ani}}(r)\rho_*(r)\sigma_{\mathrm{r}}^2(r)}{r} = -\rho_*(r)\frac{\partial \Phi(r)}{\partial r}, \tag{10}$$

with the stellar anisotropy parameterized as

$$\beta_{\mathrm{ani}}(r) \equiv 1 - \frac{\sigma_{\mathrm{t}}^2(r)}{\sigma_{\mathrm{r}}^2(r)}. \tag{11}$$

The mass-sheet transform (MST) is a multiplicative transform of the lens Equation (Eqn. 1) (Falco et al. 1985)

$$\lambda \boldsymbol{\beta} = \boldsymbol{\theta} - \lambda \boldsymbol{\alpha}(\boldsymbol{\theta}) - (1 - \lambda)\boldsymbol{\theta}, \tag{20}$$

$$\kappa_\lambda(\theta) = \lambda \times \kappa(\theta) + (1 - \lambda)$$

TDCOSMO IV
S Birrer et al. 2020

The Hubble constant, when inferred from the time-delay distance, $D_{\Delta t}$, transforms as (from Eqn. 9)

$$H_{0\lambda} = \lambda H_0. \tag{29}$$

Mathematically, all the MSTs can be equivalently stated as a change in the angular diameter distance to the source

$$D_{\mathrm{s}} \to \lambda D_{\mathrm{s}}. \tag{30}$$

We model the PSF of HST and KCWI images with MGE

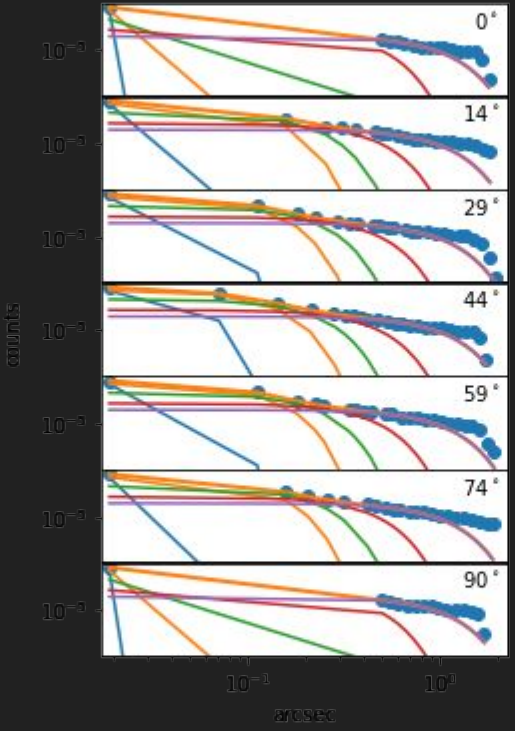

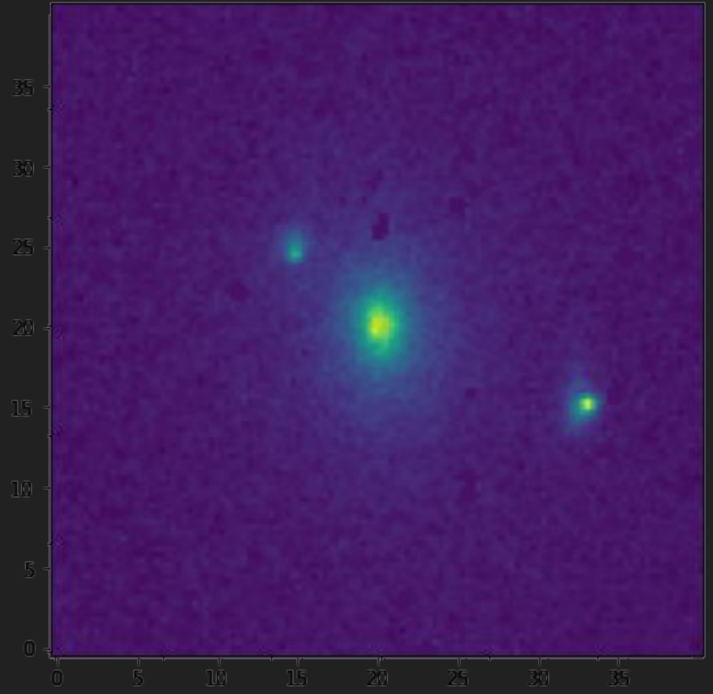

Knabel et al. in prep